Computer Communications 36 (2013) 342–350

Contents lists available at SciVerse ScienceDirect

Computer Communications

journal homepage: www.elsevier.com/locate/comcom

Multi-domain integrated grooming algorithm for green IP over WDM network

Weigang Hou, Lei Guo *, Xiaoxue Gong, Zhimin Sun

College of Information Science and Engineering, Northeastern University, Shenyang 110819, China

ARTICLE INFO

Article history:
Received 28 March 2012
Received in revised form 17 July 2012
Accepted 24 September 2012
Available online 2 October 2012

Keywords:
Multi-domain IP over WDM network
Power efficiency
Port savings
Green grooming

ABSTRACT

With the continuous expansion in the network scale and growing popular Internet applications, the sharply increasing electrical consumption and even carbon dioxide emissions have became bottlenecks of the future network development. Consequently, *greening network* comes to a very important issue. Foremost, ensuring the scalability and robustness, we divide the network into multiple domains for the distributed routing and management. As these tendencies undergo widespread attentions, providing solutions for multi-domain green networks are of the utmost importance. This paper enables the power conservation in multi-domain IP over WDM networks by means of presenting a power- and port-cost- efficient approach. This approach delves into power-efficient channel provisions of connection demands and an effective integration of the hybrid grooming and the waveband merging. For each intra-domain connection demand, our method executes the intra-domain hybrid grooming within the physical topology and updates the power efficiency of this domain in real-time. For each inter-domain connection demand, through link-cost adjustments, our method first computes the loose route which is the most power-efficient path from the source border node to the destination border node within the logical topology. The link-cost adjustment aims to make the loose route traverse over higher power-efficient domains and logical links. Next, it orderly performs the intra-domain hybrid grooming between two selected border nodes in each traversed domain of this loose route, from the source node to the selected border node in the source domain and from the selected border node to the destination node in the destination domain. In final, within each single domain, our method merges several full-loaded lightpath segments into a single waveband tunnel along with more than two physical hops by the intra-domain waveband merging. The Optical Cross-Connect (OXC) ports are able to be further saved. In comparison to the traditional multi-domain grooming approach, our method exhibits the higher power efficiency and port savings.

1. Introduction

Switching demands electrically on IP layer requires marginal router power at all of immediate nodes, while promisingly, one practical method embedded by an IP over Wavelength-Division-Multiplexing (WDM) network can overcome this drawback. It is called the hybrid grooming and it has two key components [1]: (a) the traffic grooming migrates multiple IP-level demands into a high-capacity lightpath to reduce electrical Transmission Ports (TPs), and (b) the optical bypass ensures a lightpath can be switched as an All-optical (OOO) single unit without having any intermediate Optical-Electrical-Optical (OEO) conversions. As a consequence, the power consumed by router ports and OEO operations are thereby greatly decreased. As shown in Fig. 1, on the upper IP layer, the electrical switching consumes twelve TPs (i.e., ports 1–12). Nevertheless, based on the hybrid grooming, these demands from IP layer are multiplexed into the lightpath and switched as an entity (i.e., the solid line on WDM optical layer of Fig. 1). Accordingly, the traversed devices have been replaced from power thirsty routers to Optical Cross-Connects (OXCs) whose power consumptions are negligible. On the basis of assumption above, the hybrid grooming provides the saved power from twelve TPs in comparison to the electrical switching. On the other hand, comparing with the traffic grooming without any optical bypass (i.e., the dashed line of Fig. 1), two Grooming Matrix Ports (GMPs) (i.e., ports 22 and 23) and two transceivers (i.e., transceivers 18 and 19) are saved. However, in the process of executing the hybrid grooming, the power consumed by establishing lightpaths is the performance penalty. In Fig. 1, for instance, the power of six aggregating ports (i.e., ports 33–38), two GMPs (i.e., ports 21 and 24), and two transceivers (i.e., transceivers 17 and 20) are consumed. This observation motivates us to place significant attentions on a novel aspect of the hybrid grooming, and it is the power efficiency [2]. Without losing a generality, a power-efficient IP over WDM network should be the network that can save more

* Corresponding author. Address: P.O. Box 365, College of Information Science and Engineering, Northeastern University, Shenyang 110819, China. Tel./fax: +86 24 83684219.

E-mail address: haveball@263.net (L. Guo).

0140-3664/$ - see front matter © 2012 Elsevier B.V. All rights reserved.
http://dx.doi.org/10.1016/j.comcom.2012.09.013

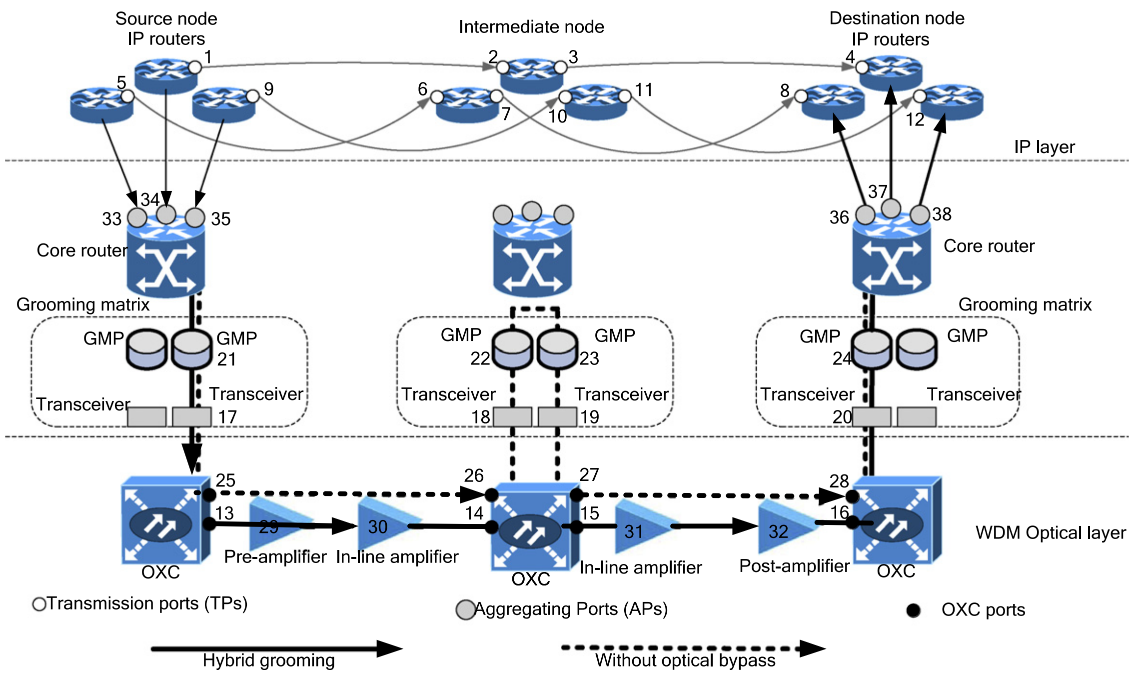

Fig. 1. Hybrid grooming in IP over WDM networks.

power with the hybrid grooming at the slightly additional cost of the power consumed by establishing lightpaths. Currently, there are two main approaches of implementing the hybrid grooming [3]: (a) only the single-hop lightpath segment can be found to carry demands, which we call the single-hop hybrid grooming and (b) several lightpath segments (at least one) are cascaded hop-by-hop for carrying demands, and each lightpath segment is not confined to the newly-found one, it can also be the established one. Approach (b) is called the multi-hop hybrid grooming. Our previous work [2] has exhibited the better power efficiency of the latter, and in the following parts of this study, we directly call the approach (b) as "*hybrid grooming*" for simplicity.

On the other hand, for the purpose of security and scalability in a multi-domain optical network, the single domain operator shares scarce information resource with the others from the different domains. Furthermore, the accurate information of physical topologies and link states is not within the scope of the inter-domain information exchange. In other words, the partial information oriented and inter-domain hybrid grooming is not easily implemented in the whole network through the single stepping. This unique characteristic makes the multi-domain hybrid grooming for the power efficiency become a more complex issue. Fig. 2 exhibits the physical topology of a typical multi-domain optical network, wherein two types of physical links are involved: the intra-domain link denoted as a thin line and the inter-domain link of a coarse line. Two nodes within the same domain are connected by an intra-domain link while the inter-domain link is built between two border nodes (i.e., dark circles) of its two adjacent domains. Each border node has the knowledge of both its located domains' physical topology and the global information of physical link states, while the other interior nodes exclusively know the local information.

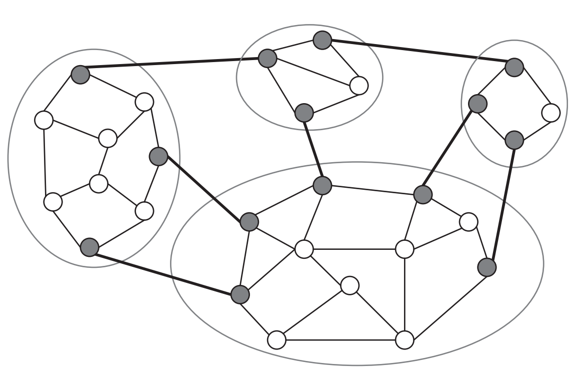

Fig. 2. The physical topology of a multi-domain optical network.

As performed in the previous work [4], we require making the abstraction of the global topology to form a two-layered topology structure. This structure includes an abstracted logical topology on high layer and independent and single-domain physical topologies on low layer, shown in Fig. 3. The full-mesh scheme is adopted to enable the topology abstraction. In detail, we find at most K ($K \geqslant 1$) different shortest paths as a group for each border node pair within every domain in Fig. 2, and each path group is abstracted into a logical link (denoted as a dashed line on the high layer of Fig. 3). One member of the path group also belongs to the respective logical link and is known as the logical sub-link. Owing to the tight relationship between the saved power of the hybrid grooming and the number of physical routing hops [5], each link of Fig. 2 has one unit of cost in the case of exploiting the full-mesh scheme described above. Hereafter, on the high layer of Fig. 3, each domain has been changed into a meshed area that includes its own logical links and border nodes, and the global multi-domain physical topology has became into a logical one that includes all of logical links, border nodes and inter-domain links; on the low layer of Fig. 3, the global multi-domain physical topology has been divided into several independent and single-domain physical topologies.

1.1. Related works

Zhu [6] first estimated the Bit-Error-Rate (BER) evolution of mixed regenerator operations by their analytical model, and then addressed the cost- and power-efficient design in translucent optical networks based on the estimation above. This approach

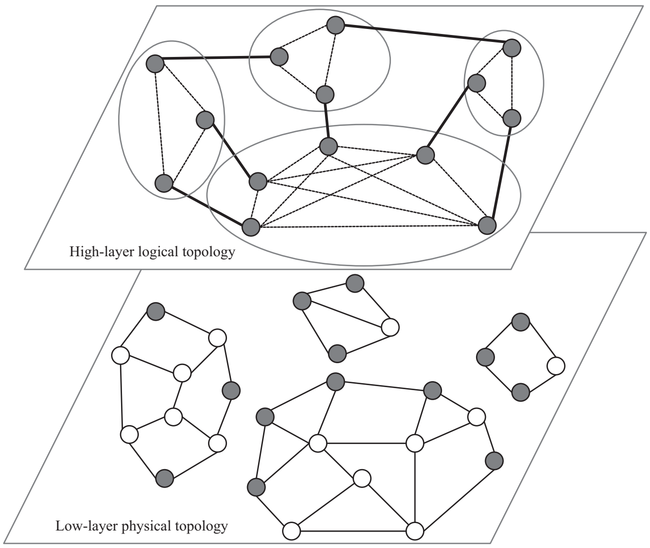

Fig. 3. Two-layered topology structure converted from Fig. 2.

effectively reduced the cost and power consumption of translucent networks via replacing some of OEO 3R regenerators with OOO 2R ones. Meanwhile, the end-to-end optical signal quality was still maintained. For the transparent WDM optical network, Angelo [7] proposed a power-aware routing and wavelength assignment algorithm known as Load Based Cost (LBC). The LBC improved the overall power efficiency by shutting down as many unused optical amplifiers as possible. Moreover, a modified version of the First Fit (FF) wavelength assignment was also entailed in LBC to realize the further power efficiency improvements. With aim to save power in IP-over-WDM networks featuring time-of-the-day traffic variation, Zhang et al. [8] presented a novel approach of shutting down idle line cards and chassis owned by routers from the Mixed Integer Linear Programming (MILP) model to heuristics. Meanwhile, the amount of network element reconfigurations and re-routings caused by the traffic disruption were both minimized. Chen and Jaekel [9] detailed a power-efficient hybrid grooming with the awareness of demand holding times. An ILP formulation was also described for minimizing the component power consumption under both static and dynamic cases. The static router-port power reduction was enabled by the sub-wavelength multiplexing while the dynamic power undergoes reduction via minimizing the amount of electrical switching. The power savings brings up to 7%–40% gain by utilizing the knowledge of demand holding times. Another time-aware hybrid grooming for the power minimization was proposed by Zhang et al. [10]. They formulated an ILP model for the power reduction under the static case where all connection demands with their setup and tear-down times were known in advance. On the other hand, a layered graph-based grooming heuristic with the time awareness was also taken into account for the dynamic case. Observed from simulation results, the Time Aware Traffic Grooming (TATG) exhibited the least power consumption when the traffic load was relatively low. Similarly, Xia et al. [11] also presented a novel auxiliary graph-based grooming scheme to minimize the total operational power. The auxiliary graph captured the power consumption of each provisioning operation. Performance evaluation demonstrated that the scheme in [11] required the less operational power in comparison to the direct-lightpath approach. Another important conclusion was claimed that the higher power efficiency can be enabled by executing the hybrid grooming at end nodes instead of intermediate ones. Based on a tap-or-pass node architecture, Farahmand et al. [12] evaluated the performance of the lightpath extension and the lightpath dropping in terms of the optical power budget. The considerable power could be saved by using these two grooming strategies when traffic load was moderate. Meanwhile, a good trade-off between low blocking probability and high power savings was well solved. Yang and Kuipers [13] made efforts on the power-efficient path selection in IP-over-WDM optical networks along with the scheduled traffic model and exhibited the significant power savings gained by their power-aware routing algorithm with the flexible exploiting hybrid grooming.

Overall, the above works are all limited in maximizing power savings of the hybrid grooming while the power-efficiency oriented hybrid grooming is not considered yet. Without loosing a generality, a power-efficient IP over WDM network should be the network that can save more power with the hybrid grooming at the slightly additional cost of the power consumed by establishing lightpath segments. While in real-world applications, the connection demand usually arrives at the network dynamically and the traffic matrix is unknown in advance. In a word, previous and power-efficient hybrid grooming approaches are not directly applied to the multi-domain case owing to the lack of global information.

1.2. Our contributions

Based on the two-layered topology structure in Fig. 3, the main idea of our planning is described in the following. For each intra-domain connection demand, we perform the hybrid grooming for it directly in the located domain on the low layer. If this intra-domain hybrid grooming is performed successfully, we establish the connection for this demand, and then the power efficiency of this located domain is evaluated for the update. For each inter-domain connection demand, we first compute a loose route which is the most power-efficient path from the source border node to the destination border node on the logical topology where each link cost has been adjusted. In detail, the logical link cost is adjusted according to its average number of physical routing hops and traffic load. It is ensured that the logical link with a lower cost is the more power-efficient one; the inter-domain link cost is adjusted according to the average cost of all the logical links within its two adjacent domains. Similarly, the lower inter-domain link cost implies the higher power efficiency. The objective of link cost adjustments is to make our loose route traverse over the most power-efficient domains and consume the most power-efficient logical links of each domain. Next, we orderly perform the hybrid grooming for this inter-domain connection demand in its source domain, traversed domain(s) and the destination domain. In final, this inter-domain connection demand is carried by continuous lightpath segments, and the highest power efficiency can be enabled. With aim to further save more OXC ports (e.g., ports 13–16 in Fig. 1) in each domain, also to achieve the higher power efficiency once the power consumed by OXCs plays a key role in the future, the full-loaded lightpath segments are further merged into a waveband tunnel along with at least two physical routing hops via the waveband merging [14]. Due to integrating the hybrid grooming for power efficiency with the waveband merging for port savings domain-by-domain, we call this mechanism in each domain as the intra-domain integrated grooming. Therefore, the measurement of intra-domain power efficiency, the link cost adjustment for loose route computations and the implementation of intra-domain integrated grooming are our highlights.

2. Problem statements

2.1. Network model

The physical topology of a multi-domain optical network is denoted as $G(InterL, D)$ where $InterL$ represents the inter-domain link set and the physical topology set D records the physical topologies of $|D|$ domains and we have $D = \{D_r(BN_r, CN_r, IntraL_r)|r = 1, 2, \ldots, n|D|.\}$. Towards the physical topology of domain D_r, the notations BN_r, E_t and $IntraL_r$ are the border node set, interior node set and the intra-domain link set, respectively. The high layer logical topology is denoted as $G_v(InterL, D^v)$, where the logical topology set D^v records logical topologies (i.e., meshed areas) of $|D|$ domains and we have $D^v = \{D^v_r(BN_r, VL_r)|r = 1, 2, \ldots, |D|\}$. Towards each meshed area of domain D_r, E_{TP} is the logical link set. Other important parameters and decision variables are introduced in the following.

2.2. Parameters

P_t is the power consumed by each transceiver;
P_{gmp} is the power consumed by each grooming matrix port;
P_a is the power consumed by each optical amplifier;
P_{AP} is the power consumed by each (de)-aggregating port;
P_{TP} is the power consumed by each transmission port of the IP router;
LP^r is the set of established lightpath segments of domain D_r;
CR^r is the set of successfully groomed intra-domain connection demands of domain D_r;
ACR^r is the set of successfully groomed inter-domain connection demands added at the domain D_r;
DCR^r is the set of successfully groomed inter-domain connection demands dropped at the domain D_r;
ICR is the set of successfully groomed inter-domain demands of the whole multi-domain optical network;
W is the set of available wavelengths on each intra-domain link;
W_C is the wavelength capacity;
d is the distance between two adjacent in-line optical amplifiers;
$D_{i,j}$ is the distance of the physical link (i, j), and the case $D_{i,j} \geqslant d$ should be satisfied;
$LP_{y,x,z}$ is the lightpath segment with consuming the wavelength λ_y $(1 \leqslant y \leqslant |W|)$ from node x $(x \in BN_r \cup CN_r)$ to node z $(z \in BN_r \cup CN_r)$;
$LP^t_{y,x,z}$ is the number of connection demands carried by the lightpath segment $LP_{y,x,z}$;
$H_{y,x,z}$ is the number of physical routing hops of the lightpath segment $LP_{y,x,z}$;
$VL^r_{x',z'}$ is the logical link between the border node $x'(x' \in BN_r)$ and the border node $z'(z' \in BN_r)$ of domain D_r, $VL^r_{x',z'} \in VL_r$;
$SVL^r_{x',z',m}$ is the mth logical sub-link belongs to $VL^r_{x',z'}$ of domain D_r;
$PH^r_{x',z',m}$ is the number of physical routing hops of the logical sub-link $SVL^r_{x',z',m}$;
$PT^r_{x',z',m}$ is the traffic load of the logical sub-link $SVL^r_{x',z',m}$;
$TB_{i,j}$ is the used bandwidth of the physical link (i, j);
$|\Omega|$ is the number of elements in set Ω.

2.3. Decision (Boolean) variables

$\gamma^{i,j}$ is 1 when the physical link (i, j) is consumed by one lightpath segment; otherwise it is 0.
β^i is 1 when the node i is selected as the source-end node of one lightpath segment; otherwise it is 0.
φ^i is 1 when the node i is selected as the destination-end node of one lightpath segment; otherwise it is 0.
$\gamma^{i,j}_{y,x,z}$ is 1 when the physical link (i, j) is consumed by the lightpath segment $LP_{y,x,z}$; otherwise it is 0.
$\gamma^{i,j,r}_{x',z',m}$ is 1 when the physical link (i, j) is consumed by the logical sub-link $SVL^r_{x',z',m}$; otherwise it is 0.

2.4. Quantitative model of the intra-domain power efficiency

The intra-domain power efficiency reflects a correlation between the power consumed by establishing lightpath segments PC^r and the power saved with the hybrid grooming SP^r of the domain D_r. Among which, PC^r has the traffic-independent part PC^r_0 and the traffic-dependent part PC^r_t, that is:

$$PC^r = PC^r_0 + PC^r_t \tag{1}$$

In Eq. (1), the value of PC^r_0 mainly depends on the number of lightpath segments established in the domain D_r, then we have:

$$PC^r_0 = PC^r_{EDFA} + 2 \times |LP^r| \times (P_t + P_{gmp}) \tag{2}$$

In Eq. (2), the PC^r_{EDFA} records the total power consumed by optical amplifiers of the domain D_r and can be computed in the following:

$$PC^r_{EDFA} = \sum_{i \in BN_{r \cup CN_r}} \sum_{j \in BN_{r \cup CN_r}, j \neq i} \{\lceil (\gamma^{i,j} \cdot D_{i,j})/d \rceil - 1\} \times P_a + P_a \times \left(\sum_{i \in BN_{r \cup CN_r}} \beta^i + \sum_{i \in BN_{r \cup CN_r}} \varphi^i \right) \tag{3}$$

The first half of Eq. (3) statistics the total power consumed by in-line optical amplifiers while the other half is the total power consumed by pre- and post-amplifiers of the domain D_r .
In terms of PC^r_t, the more demands processed in the domain D_r brings with the bigger PC^r_t, then we have:

$$PC^r_t = 2 \times P_{AP} \times |CR^r| + P_{AP} \times (|ACR^r| + |DCR^r|) \tag{4}$$

In this study, the power consumed by wavelength conversions is negligible and performed by pre-configured transceivers at end nodes of established lightpath segments. In other words, the power consumed by transceivers, which has been evaluated in Eq. (2), has involved this part of power consumption.
On the other hand, the power saved with the hybrid grooming SP^r in the domain D_r also has two main parts, they are the saved power from transmission ports of IP routers SP^r_{tp}, and the saved power from OEO conversions SP^r_{oeo}, then we have:

$$SP^r = SP^r_{tp} + SP^r_{oeo} \tag{5}$$

By using the hybrid grooming in the domain D_r, the more connection demands carried by lightpath segments and the longer OOO transmission distance provide the higher SP^r_{tp}, which is thereby presented in the following

$$SP^r_{tp} = 2 \cdot P_{TP} \cdot \sum_{y \in W} \sum_{x \in BN_r \cup CN_r} \sum_{z \in BN_r \cup CN_r, z \neq x} LP^t_{y,x,z} \times H_{y,x,z} \tag{6}$$

$$H_{y,x,z} = \sum_{i \in BN_{r \cup CN_r}} \sum_{j \in BN_{r \cup CN_r}, j \neq i} \gamma^{i,j}_{y,x,z} \quad \forall x, z \in BN_r \cup CN_r, \quad \forall y \in W \tag{7}$$

The saved power from OEO conversions SP^r_{oeo} is only proportional to OOO transmission distances of lightpath segments in the domain D_r. Then we have:

$$SP^r_{oeo} = 2 \cdot (P_t + P_{gmp}) \cdot \sum_{y \in W} \sum_{x \in BN_r \cup CN_r} \sum_{z \in BN_r \cup CN_r, z \neq x} (H_{y,x,z} - 1) \tag{8}$$

Without losing a generality, a more power-efficient domain should use the hybrid grooming to save considerable power at the slightly additional cost of the power consumption of establishing lightpath segments. Consequently, we entail an important metric PR^r, which we call the power ratio, to evaluate the intra-domain power efficiency of the domain D_r in the following.

$$PR^r = PC^r / SP^r \tag{9}$$

Intuitively, a smaller PR^r implies a higher power efficiency of the domain D_r. Accordingly, the optimization objective of this study is to minimize the overall power ratio PR owned by the entire network, which can be described as follows:

$$Minimize\, PR = \left\{ \sum_{r=1}^{|D|} PC_0^r + 2 \times P_{AP} \times \left[\left(\sum_{r=1}^{|D|} |CR^r| \right) + |ICR| \right] \right\} \Big/ \left(\sum_{r=1}^{|D|} SP^r \right) \tag{10}$$

3. Algorithm description

3.1. Link cost adjustments

3.1.1. Logical link cost adjustment

As mentioned in Section 1, after we perform the full-meshed scheme, in the meshed area mapped into the initial domain D_r, each logical link $VL^r_{x',z'}$ has a path group with an actual size of $M(1 \leqslant M \leqslant K)$. Consequently, in terms of $VL^r_{x',z'}$, the values of number of physical routing hops $VLH^r_{x',z'}$ and the traffic load $VLT^r_{x',z'}$ should be on average of corresponding values owned by its logical sub-links. Then, we have:

$$VLH^r_{x',z'} = \frac{\sum_{m=1}^{M} PH^r_{x',z',m}}{M}, \quad \forall x', z' \in BN_r \tag{11}$$

$$PH^r_{x',z',m} = \sum_{i \in BN_{r \cup CN_r}} \sum_{j \in BN_{r \cup CN_r}, j \neq i} \gamma^{i,j,r}_{x',z',m}, \quad \forall x', z' \in BN_r, \quad \forall m \in \{1, M\} \tag{12}$$

$$VLT^r_{x',z'} = \frac{\sum_{m=1}^{M} PT^r_{x',z',m}}{M}, \quad \forall x', z' \in BN_r \tag{13}$$

$$PT^r_{x',z',m} = \frac{\frac{1}{W_C \cdot |W|} \cdot \sum_{i \in BN_{r \cup CN_r}} \sum_{j \in BN_{r \cup CN_r}, j \neq i} \gamma^{i,j,r}_{x',z',m} \cdot TB_{i,j}}{PH^r_{x',z',m}}, \quad \forall x', z' \in BN_r, \quad \forall m \in \{1, M\} \tag{14}$$

As mentioned in our previous work [5], the saved power is proportional to both OOO transmission distances and the number of connection demands carried by lightpath segments. Under this viewpoint, with aim to make a loose route select more power-efficient logical links, we adjust the logical link cost according to the following principle:

$$Cost_{VL^r_{x',z'}} = \frac{1}{\alpha_1 \cdot VLH^r_{x',z'} + \alpha_2 \cdot VLT^r_{x',z'}} \tag{15}$$

where, α_1 and α_2 are routing hop number and traffic load adjustment coefficients, respectively. Meanwhile, the conditions $0 \leqslant \alpha_1,\ \alpha_2 \leqslant 1$ and $\alpha_1 + \alpha_2 = 1$ are both satisfied. Eq. (15) tells us the logical link along with more physical routing hops and higher traffic load has a lower cost, which makes it tend to be selected during the loose route computation.

3.1.2. Inter-domain link cost adjustment

Similarly, in order to let a loose route traverse more power-efficient domains, we need to adjust the inter-domain link cost according to values of power ratios in its two adjacent domains. In other words, the higher power efficiency (i.e., lower power ratio) of adjacent domains, the lower cost is assigned to the corresponding inter-domain link. We can infer that from Eq. (15), once logical links in a domain are assigned by lower costs, their domain will be more power efficient. Based on this principle, the inter-domain link cost is thereby the average cost of logical links from its two adjacent domains. Then we have:

$$Cost_{(r1^*, r2^*)} = \delta_1 \cdot \frac{\sum_{x' \in BN_{r1^*}} \sum_{z' \in BN_{r1^*}} Cost_{VL^{r1^*}_{x',z'}}}{|VL_{r1^*}|} + \delta_2 \cdot \frac{\sum_{x' \in BN_{r2^*}} \sum_{z' \in BN_{r2^*}} Cost_{VL^{r2^*}_{x',z'}}}{|VL_{r2^*}|} \tag{16}$$

where, r_1^* and r_2^* are adjacent domain indexes and the condition $1 \leqslant r_1^*, r_2^* \leqslant |D|$ is satisfied. Similarly, δ_1 and δ_2 are adjustment coefficients, and both $0 \leqslant \delta_1, \delta_2 \leqslant 1$ and $\delta_1 + \delta_2 = 1$ are satisfied.

3.1.3. Power efficiency benefits

We will be further aware of power efficiency benefits made by link cost adjustments on the logical topology in the following instance. Given a logical topology generated by the full-mesh scheme in Fig. 4, we first decide the source and the destination border nodes for the inter-domain connection demand. In the source domain, we compute shortest paths from the source node of the inter-domain connection demand to all of border nodes in the source domain, and wherein, the destination node of the least-cost path is the source border node of the loose route (G1 in Fig. 4). Similarly, we can determine the destination border node, (G7 in Fig. 4)

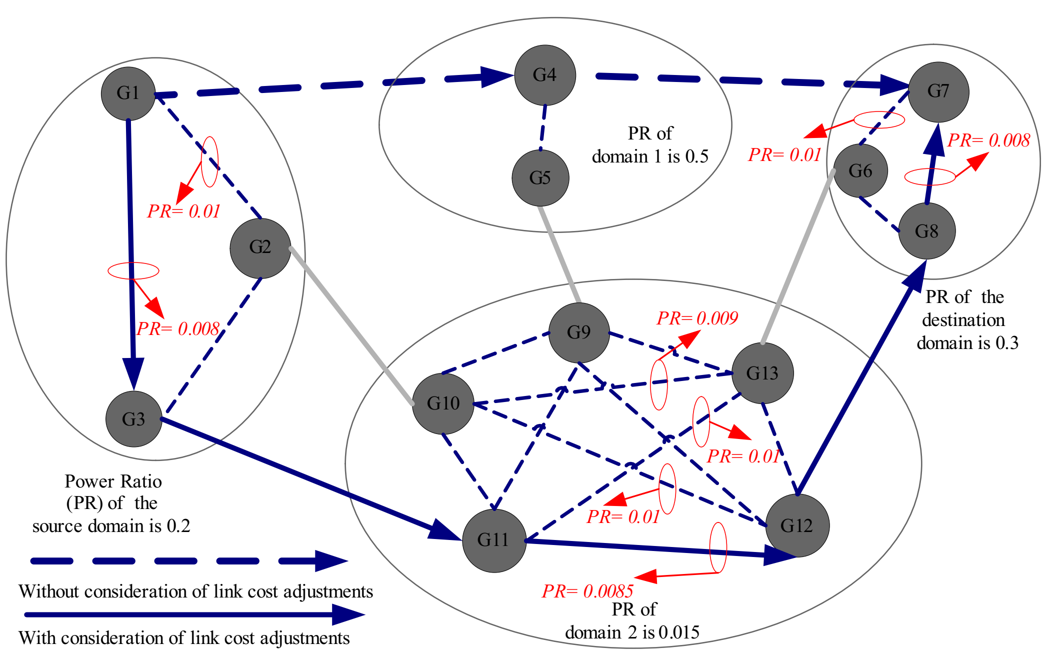

Fig. 4. Instance of power efficiency benefits made by link cost adjustments.

which is the source node of the least-cost path in the destination domain. Regardless of link cost adjustments, the final loose route is G1 → G4 → G7 because all of inter-domain links and logical links have the same cost and the loose route along with the least number of physical routing hops is our decision. Nevertheless, the power ratio of the traversed domain (i.e., domain 1 in Fig. 4) is 0.5, which implies that the power efficiency of domain 1 is the lowest in the whole multi-domain optical network because power ratios of the others are all smaller than 0.5. On the contrary, after link cost adjustments, the final loose route G1 → G3 → G11 → G12 → G8 → G7 is determined because its consumed inter-domain links and logical links have the lowest costs corresponding to the smallest power ratios (for instance, the logical link (G11, G12) has the lowest adjusted cost corresponding to the smallest power ratio 0.0085 in domain 2 and the inter-domain link (G3, G11) has the lowest adjusted cost because power ratios of its two adjacent domains are the lowest). As a consequence, the lowest power-efficient loose route G1 → G4 → G7 is not determined and the result is the overall improved power efficiency for the multi-domain optical network. We can see that from this instance above, the adjusted cost of inter-domain link mainly decides which domain is traversed by the final loose route, while the adjusted cost of the logical link decides which border node is the ingress or egress one in each traversed domain.

3.2. Intra-domain integrated grooming

After the loose route is determined, we orderly perform the intra-domain integrated grooming within the source domain, the destination domain and the other traversed domains of the loose route. Prior to this, it is required to construct an Intra-domain Integrated Grooming Graph (I2G2) as performed in our previous work [14] and to compute each shortest path in the Wavelength Integrated Auxiliary Graph (WIAG) of I2G2 as follows: in view of the source domain, the shortest path should be found from the source node of the connection demand to the egress border node (i.e., the source border node); with regard to the destination domain, the shortest path should be found from the ingress border node (i.e., the destination border node) to the destination node of the connection demand; in terms of each traversed domain, its own shortest path should be found from the ingress border node to the egress border node. Only if all of shortest paths are successfully found, the intra-domain integrated grooming can be performed domain-by-domain and this technique includes two main operations of the intra-domain hybrid grooming and the intra-domain waveband merging.

3.2.1. Intra-domain hybrid grooming

Take an example of the source domain in Fig. 4, the corresponding physical topology can be found in the lower part of Fig. 3. Then, the WIAG of the source domain can be constructed by both node- and link-level mappings from this physical topology as performed in our previous work [14]. Each virtual node on the Lightpath Virtual Topology (LVT) is connected with its corresponding wavelength nodes on $|W|$ wavelength planes via virtual links. Based on the source-domain WIAG, we compute the shortest path from the virtual node corresponding to the source node, then to the virtual node corresponding to the border node G1 and destined for the virtual node corresponding to the border node G3. Referenced by [14], there are four types of paths vary along with the different network resource states during the phase of executing the intra-domain hybrid grooming:

(1) The wavelength path on the wavelength plane, and then a new lightpath will be established on LVT as well as two transceivers will be consumed. Meanwhile, the number of consumed OXC ports is $2 \times (H + 1)$, where H is the number of physical routing hops owned by this wavelength path. The OEO ports are negligible in this study because wavelength conversions are enabled by transceivers; (2) the single-hop lightpath segment on LVT, and (3) several continuous lightpath segments on LVT. No one transceiver or transmission port is consumed by these two kinds of paths; (4) the multi-hop path which is combined with cascade lightpath segments on LVT and wavelength paths on wavelength planes. In (4), once a wavelength path is determined, the number of its consumed OXC ports is also $2 \times (H + 1)$ and two transceivers are used. While for paths on LVT, no one transceiver or OXC port is consumed.

3.2.2. Intra-domain waveband merging

We update the LVT information in real-time, especially for the spare bandwidth of established lightpath segments on LVT. Once a lightpath segment has no remaining bandwidth, we find physical links of its wavelength path. And then, via link-level mappings, waveband segments are established on the corresponding wave-Band Virtual Topology Plane (BVTP) in the waveBand Layered Graph (BLG) of I2G2. If more than two continuous waveband segments are overlapped, the current total number of consumed OXC ports N_p should be updated and we have $N_p = N_p - 2 \times N'$, where N' denotes the times of overlapping.

3.2.3. Time complexity analysis

We consider time complexities of routing connection demands on the high layer logical topology and the corresponding intra-domain physical topology in the worst case, respectively. Because we run the shortest path algorithm, the time complexities described above are both mainly dependent on the times of running Dijkstra's. In view of the loose route computation on the high layer logical topology, we have the time complexity $TC_1 = \sum_r |BN_r|^2$; while for the intra-domain hybrid grooming in domain D_r, we have the time complexity $TC_2 = (|W| + 1) \times (|BN_r| + |CN_r|)^2$.

4. Simulation analysis

In Fig. 5, the test topology has the multi-domain structure combined with three small-size regions (i.e., RedIRIS, NSFnet, and GEANT), each of which has six border nodes. Meanwhile, 9 inter-domain links are configured in our test topology. Each link has one unit of physical distance (1 km). The source and destination nodes of each connection demand are randomly generated and the required bandwidth is always one granularity unit (i.e., OC-1). Each connection demand arrives according to an independent Poisson process with the arrival rate β and the demands' holding times is negatively exponentially distributed $1/\mu$, i.e., the network load is β/μ Erlang. In simulations, we set μ to 1. If we cannot find eligible path for the connection demand, this demand is abandoned immediately. All simulation results are obtained by generating up to 10^3 connection demands. The initial number of available transceivers on each interior node $|T| = 12$, and each border node has enough transceivers (i.e., $|T| = 100$). The initial number of available wavelengths on each intra-domain link $|W| = 12$. The other parameter settings are: $K = 4$, $P_t = P_{gmp} = 73$ (W) [15], $P_a = 8$ W [15], $P_{AP} = P_{TP} = 1000$ W [15], W_C = OC-4, $\delta_1 = \delta_2 = 0.5$ and $d = 0.25$ km. We compare performances of average port cost, total saved power SP and the overall power ratio PR between the traditional Multi-Domain Grooming (MDG) [4] and our method known as Power-Aware Multi-Domain Grooming (PA-MDG). Wherein, PR can be computed in Eq. (10) and SP is evaluated as follows:

$$SP = \left(\sum_{r=1}^{|D|} SP^r \right) \tag{17}$$

Meanwhile, because the higher power efficiency could be determined through our link-cost adjustments, the potential negative effect on the link transmission delay should be checked according

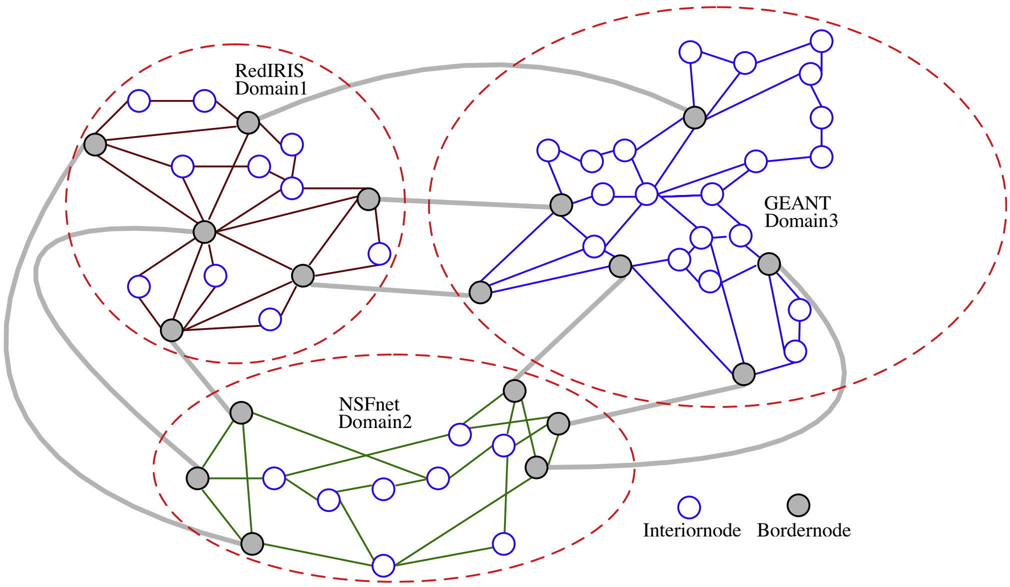

Fig. 5. The test topology.

to compared results between our PA-MDG and the traditional MDG. In this paper, the link transmission delay per 1 km is 5 µs [16]. Therefore, the total transmission delay can be evaluated as follows:

$$\omega \cdot \sum_{r=1}^{|D|} \left(\sum_{y \in W} \sum_{x \in BN_r \cup CN_r} \sum_{z \in BN_r \cup CN_r, z \neq x} H_{y,x,z} \right) \tag{18}$$

Similarly, in order to check whether our link-cost adjustments make the negative effect on the network throughout, we compare the performance of blocking ratio between our PA-MDG and the traditional MDG method.

4.1. Optimal adjustment coefficients group

By means of simulations, the optimal group of adjustment coefficients (α_1, α_2) can be observed when the most power-efficient network status is determined in our PA-MDG. When the arrival rate β is given, we have the different overall power efficiency values varied from the different groups of adjustment coefficients settings (i.e., the range of the routing hop number adjustment coefficient α_1 is from 0.1 to 0.9 and the traffic load adjustment coefficient α_2 is from 0.9 to 0.1). The simulation results in Table 1 demonstrate that, the different arriving rates provide various optimal groups of adjustment coefficients. Foremost, in each optimal group, the value of α_1 is usually bigger than 0.5. It implies that, the power efficiency is more inclined to be effected by the number of physical routing hops not the traffic load.

4.2. Port savings

When optimal groups of adjustment coefficients are given (numbers beside red arrows in Fig. 6), we compare the Average Port Cost (APC), which is the ratio of the total port cost over the number of accepted connection demands, between our PA-MDG regardless of the waveband merging and our PA-MDG along with the waveband merging. In this part, we assume each OXC port has one unit of cost. The simulation results in Fig. 6 tell us that, our PA-MDG with considering the waveband merging is able to provide the further reduction of OXC ports because it continuingly merges several established lightpath segments into the waveband tunnel along with at least two physical routing hops and this port

Table 1
Optimal adjustment coefficients group.

Arrive rate (Erlang)	Optimal adjustment coefficients group	Arrive rate (Erlang)	Optimal adjustment coefficients group	Arrive rate (Erlang)	Optimal adjustment coefficients group
20	(0.8,0.2)	44	(0.8,0.2)	68	(0.6,0.4)
22	(0.8,0.2)	46	(0.8,0.2)	70	(0.9,0.1)
24	(0.8,0.2)	48	(0.8,0.2)	72	(0.7,0.3)
26	(0.8,0.2)	50	(0.7,0.3)	74	(0.7,0.3)
28	(0.8,0.2)	52	(0.9,0.1)	76	(0.7,0.3)
30	(0.6,0.4)	54	(0.7,0.3)	78	(0.9,0.1)
32	(0.6,0.4)	56	(0.7,0.3)	80	(0.8,0.2)
34	(0.6,0.4)	58	(0.9,0.1)	82	(0.9,0.1)
36	(0.9,0.1)	60	(0.9,0.1)	84	(0.9,0.1)
38	(0.9,0.1)	62	(0.6,0.4)	86	(0.9,0.1)
40	(0.9,0.1)	64	(0.9,0.1)	88	(0.9,0.1)
42	(0.9,0.1)	66	(0.9,0.1)	90	(0.9,0.1)

savings is further overall improved with increasing values of waveband granularities (waveband granlarity means the most number of wavelengths that can be merged into each waveband tunnel).

4.3. Power efficiency

When optimal groups of adjustment coefficients are given (numbers beside red arrows in Fig. 7), the overall power ratio is compared between our PA-MDG and the traditional MDG algorithm [4] in Fig. 7. The simulation results tell us that, the overall power ratio is lower than do the traditional MDG approach. In other words, exploiting our method determines the higher power efficiency. The reason for this is that, by means of our link cost adjustments, each loose route is able to traverse over the most power-efficient domains and to consume the most power-efficient logical links. Accordingly, our PA-MDG thereby saves more power compared with the traditional MDG algorithm, which can be observed in Fig. 8.

4.4. Average delay comparison

When optimal groups of adjustment coefficients are given (numbers beside red arrows in Fig. 9), we compare the average

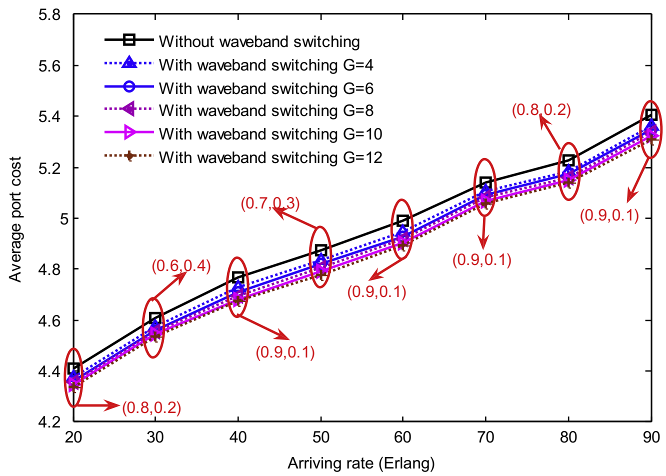

Fig. 6. Comparison of APC between our PA-MDG without the waveband merging and our PA-MDG with the waveband merging.

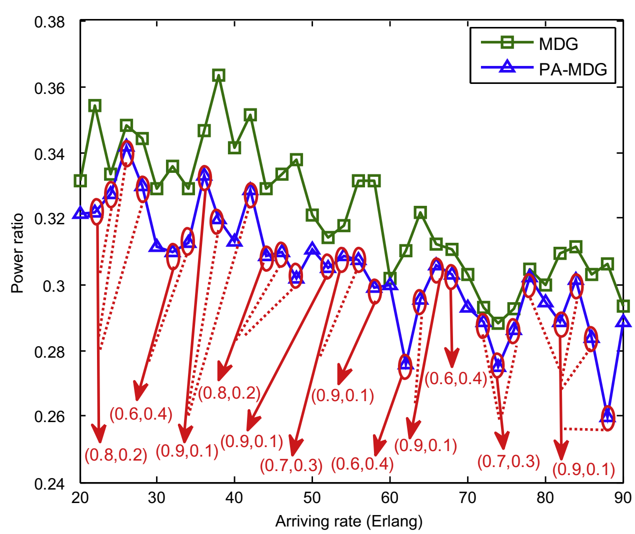

Fig. 7. Comparison of the power efficiency between our PA-MDG and the traditional MDG.

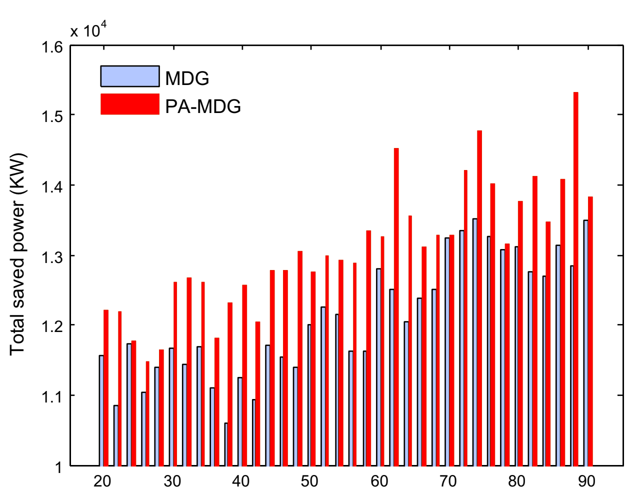

Fig. 8. Comparison of the total saved power between our PA-MDG and the traditional MDG.

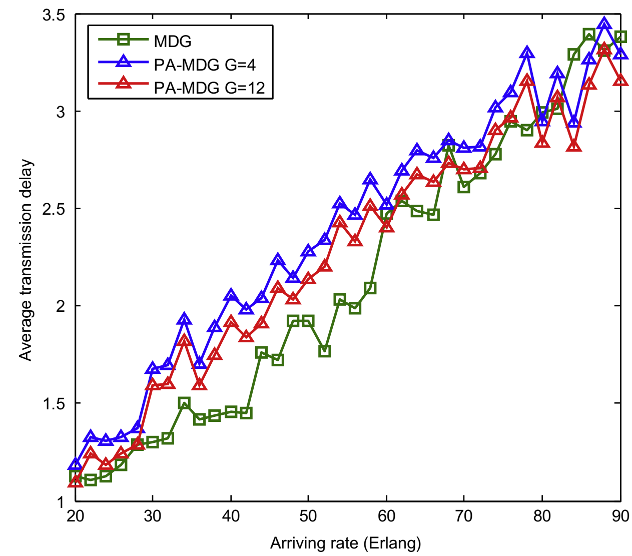

Fig. 9. Comparison of the average transmission delay between our PA-MDG and the traditional MDG.

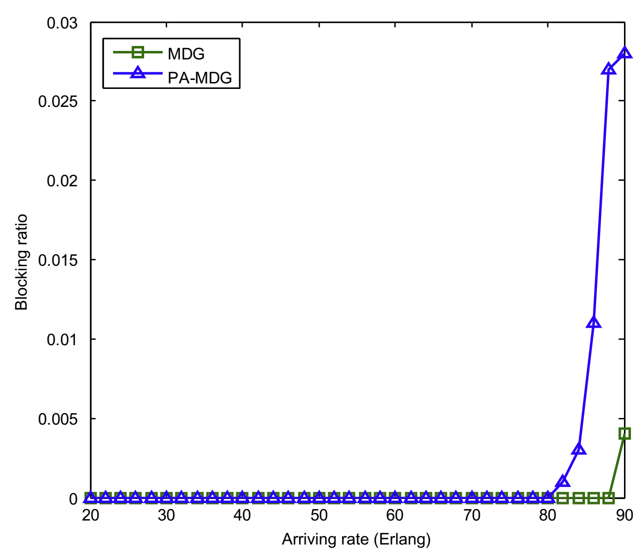

Fig. 10. Comparison of the blocking ratio between our PA-MDG and the traditional MDG.

transmission delay, which is the ratio of the total transmission delay over the number of accepted connection demands, between our PA-MDG and the traditional MDG. The simulation results demonstrate that our link cost adjustments have slightly negative effect on the average transmission delay becasue the shortest path is not always determined in our method. While several lightpath segments can be merged into a waveband and their transmission delays can be negligible in the offline state, then the negative effect above can be controled to a certain range and it can be improved with increasing values of waveband granularities.

4.5. Blocking ratio

When optimal groups of adjustment coefficients are given, we compare the blocking ratio, which is the ratio of the total number of accepted connection demands over the total number of arrived connection demands, between our PA-MDG and the traditional

MDG. We can see that in Fig. 10, in the lower network load, our method still keeps non-blocking performances in the face of the slightly negative effect caused by our link cost adjustments.

5. Conclusion

This work has addressed reasonable network resource assignments to improve the overall power efficiency in the case of multiple domains and presented a novel multi-domain integrated grooming that includes power ratio optimization, hybrid grooming and waveband merging. Our method not only has advantages of the higher power efficiency from utilizing the hybrid grooming and the higher port savings from utilizing the waveband merging, but also improves network resource assignments by designing the quantitative model for the overall power ratio. Based on the quantitative model above, we have performed link cost adjustments according to the number of physical routing hops and the traffic load, which makes the loose route traverse over the most power-efficient domains and logical links. In simulations, we have played the particular emphasis on the power efficiency, the total saved power, the average port cost, the average transmission delay and the blocking ratio of the whole network and taken the following conclusions: (1) the power efficiency is more inclined to be effected by the number of physical routing hops not the traffic load; (2) our method is more power- and port-cost-efficient in multi-domain IP over WDM networks at the slightly additional cost of the transmission delay. Therefore, our method provides valuable references of supporting the green grooming tailed for inter-domain services.

Acknowledgements

The preliminary work of this paper was presented at the International Conference on Software and Computer Applications (ICSCA) 2012. This work was supported in part by the National Natural Science Foundation of China (61172051, 61071124), the Fok Ying Tung Education Foundation (121065), the Program for New Century Excellent Talents in University (11-0075), the Fundamental Research Funds for the Central Universities (N110204001, N110604008), and the Specialized Research Fund for the Doctoral Program of Higher Education (20110042110023, 20110042120035).

References

[1] X. Wang, W. Hou, L. Guo, et al., Energy saving and cost reduction in multi-granularity green optical networks, Computer Networks 55 (3) (2011) 676–688.
[2] W. Hou, L. Guo, X. Gong, Y. Liu, Dynamic hybrid grooming based on power efficiency in green IP over WDM networks, Photonic Network Communications 23 (3) (2011) 230–245.
[3] H. Wen, R. He, L. Li, S. Wang, Dynamic grooming algorithms for survivable WDM mesh networks, Photonic Network Communications 6 (3) (2003) 253–263.
[4] X. Yang, B. Ramamurthy, Inter-domain dynamic routing in multi-layer optical transport networks, in: Proceedings of GLOBECOM, 2003, pp. 2623–2627.
[5] W. Hou, L. Guo, X. Wei, Robust and integrated grooming for power and port cost-efficient design in IP over WDM networks, Journal of Lightwave Technology 29 (20) (2011) 3035–3049.
[6] Z. Zhu, Design green and cost-effective translucent optical networks, in: Proceedings of OFC, 2011, pp. 1–3.
[7] C. Angelo, Dynamic power-aware routing and wavelength assignment for green WDM optical networks, in: Proceedings of ICC, 2011, pp. 1–6.
[8] Y. Zhang, M. Tornatore, P. Chowdhury, B. Mukherjee, Energy optimization in IP-over-WDM networks, Optical Switching and Networking 8 (3) (2011) 171–180.
[9] Y. Chen, A. Jaekel, Energy efficient grooming of scheduled sub-wavelength traffic demands, in: Proceedings of OFC, 2011, pp. 1–3.
[10] S. Zhang, D. Shen, C. Chan, Energy-efficient traffic grooming in WDM networks with scheduled time traffic, Journal of Lightwave Technology 29 (17) (2011) 2577–2584.
[11] M. Xia, M. Tornatore, Y. Zhang, P. Chowdhury, C. Martel, B. Mukherjee, Green provisioning for optical WDM networks, Journal of Selected Topics in Quantum Electronics 17 (2) (2011) 437–445.
[12] F. Farahmand, M. Hasan, I. Cerutti, J. Jue, J. Rodrigues, Power-efficient lightpath-based grooming strategies in WDM mesh networks, in: Proceedings of ICCCN, 2011, pp. 1–6.
[13] S. Yang, F. Kuipers, Energy-aware path selection for scheduled lightpaths in IP-over-WDM networks, in: Proceedings of SCVT, 2011, pp. 1–6.
[14] W. Hou, L. Guo, X. Wang, A new multi-granularity traffic grooming routing algorithm in IP over WDM networks, OPTIK – International Journal for Light and Electron Optics 122 (11) (2011) 1019–1029.
[15] G. Shen, R. Tucker, Energy-minimized design for IP over WDM networks, IEEE/OSA Journal of Optical Communications and Networking 1 (1) (2009) 176–186.
[16] B. Kantarci, H.T. Mouftah, Reliable and fast restoration for a survivable wireless-optical broadband access network, Proceedings of ICTON, 2010, pp. 1–4.